

C. S. Gardner, and N. J. Zabusky, *J. Math. Phys.* (N. Y.) **11**, 952 (1970); R. Hirota, *Phys. Rev. Lett.* **27**, 1192 (1971); P. J. Caudrey, J. D. Gibbon, J. C. Eilbeck, and R. K. Bullough, *Phys. Rev. Lett.* **30**, 237 (1973).

³R. M. Miura, C. S. Gardner, and M. D. Kruskal, *J. Math. Phys.* (N. Y.) **9**, 1204 (1968).

⁴C. S. Gardner, J. M. Green, M. D. Kruskal, and R. M. Miura, *Phys. Rev. Lett.* **19**, 1095 (1967); N. J.

Zabusky, *Phys. Rev.* **168**, 124 (1968).

⁵E. Hopf, *Commun. Pure Appl. Math.* **3**, 201 (1950); J. D. Cole, *Quart. Appl. Math.* **9**, 225 (1951).

⁶L. P. Eisenhart, *A Treatise on the Differential Geometry of Curves and Surfaces* (Dover, New York, 1960), pp. 280–290.

⁷A. R. Forsythe, *Theory of Differential Equations* (Dover, New York, 1959), Vol. VI, Chap. XXI, pp. 425–455.

Electromagnetic Instabilities, Filamentation, and Focusing of Relativistic Electron Beams

Roswell Lee and Martin Lampe

Naval Research Laboratory, Washington, D. C. 20375

(Received 12 October 1973)

We report nonlinear studies of the Weibel instability of a relativistic electron beam in a plasma. If $n_b \ll n_p$, the beam splits into self-pinched filaments at density n_p . These filaments then recombine into a single dense beam, from which the return current is expelled. The ratio of final magnetic to final streaming energy is $O(\nu/\gamma)$, and significant plasma heating occurs.

We report here on new nonlinear studies of the Weibel instability¹⁻⁴ of a relativistic electron beam propagating in a plasma. We find that the instability produces beam filamentation,⁵ plasma heating, and ultimately beam recombination into a single self-pinched non-current-neutralized filament. The beam in this final state cannot propagate if $\nu/\gamma > 1$, where ν is the number of beam electrons per classical electron radius e^2/mc^2 of beam length.

In this paper, we consider only the model of an initially homogeneous, spatially infinite, collisionless, charge- and current-neutral system, with beam propagation velocity \vec{u}_b and plasma return current flow at \vec{u}_p , along a guide field \vec{B}_z . Beams of finite cross section will be studied in a subsequent publication. We neglect ion motion, and consider only electromagnetic modes with \vec{k} normal to \vec{u}_b , $\vec{E}_{\vec{k}}$ nearly parallel to \vec{u}_b , and $\vec{B}_{\vec{k}}$ normal to both \vec{u}_b and $\vec{E}_{\vec{k}}$.

The nonrelativistic linear dispersion relation has been studied extensively.^{2,4} Relativistic corrections, we find, are straightforward. We cite here only two limiting cases of the dispersion relation. For a cold, weak beam ($\omega_b \ll \omega_p$),

$$\omega^2 = -\omega_b^2 \beta_b^2 (1 + \omega_p^2/k^2 c^2)^{-1} + \Omega_b^2, \quad (1)$$

where $\omega_j^2 \equiv 4\pi n_{0j} e^2/m\gamma_j$, $\Omega_j \equiv eB_z/m\gamma_j c$, n_j is density of species $j=b$ (beam) or p (plasma electrons), and $n_{0j} \equiv \langle n_j \rangle = n_j(t=0)$. For a weak monoenergetic beam with a Maxwellian thermal spread

$w_b \equiv \langle v_{\perp} \rangle \ll c$ of transverse velocities, and with $B_z = 0$, Vlasov theory yields

$$Z'(\omega/kw_b) = -(\omega_p^2 + k^2 c^2) \omega_b^{-2} (w_b/u_b)^2. \quad (2)$$

The waves are always purely growing. Increasing B_z stabilizes long-wavelength modes; all modes are stable if $\Omega_b > \omega_b$. Transverse beam temperature stabilizes short wavelengths (see particularly Ref. 2). Equation (2) indicates complete stability if $w_b/u_b \gtrsim \omega_b/\omega_p$, but a more accurate treatment shows continued instability at a drastically reduced growth rate.

We have used the two-dimensional relativistic, fully electromagnetic particle code RECRAD⁶ to simulate this instability. The code permits spatial variation only in the plane normal to \vec{v}_{0b} , but utilizes all three components of \vec{E} , \vec{B} , \vec{J} , and \vec{v} . Periodic boundary conditions are employed. Table I summarizes the parameters characterizing four simulations. In all cases,

TABLE I. Parameters for each of the four simulations.

Case	n_{p0}/n_{b0}	Ω_b/ω_b	w_b/u_b	γ_b
A	9	0	10^{-4}	2.5
B	9	0	0.1	2.5
C	9	0.78	10^{-4}	2.5
D	1	0	10^{-4}	1.02

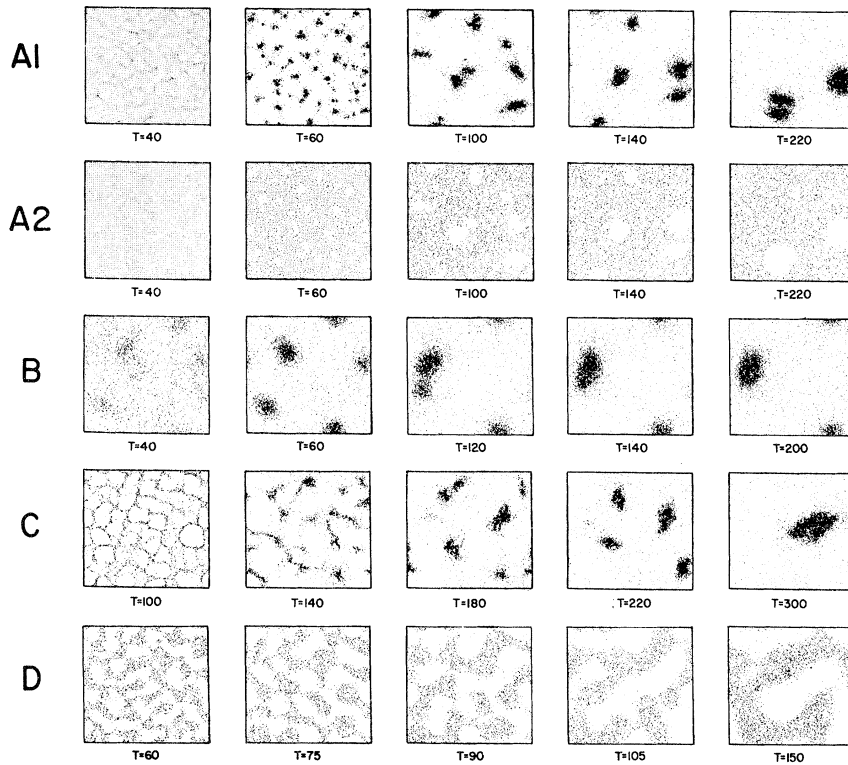


FIG. 1. Electron density in the plane normal to \vec{u}_b , at the times indicated. Row A1, beam electrons, case A; row A2, plasma electrons, case A; rows B, C, D, beam electrons, cases B, C, D.

the system is initially homogeneous and charge and current neutral, the box size is 64×64 cells, $c/\omega_p = 5$ cells, and $\nu/\gamma = 0.58$ (corresponding to one box of the periodic system).

Figure 1 shows the time development in configuration space. For cases A and B (weak, unmagnetized beam), the purely growing perturbations center on points of enhanced beam density, which magnetically attract nearby beam electrons and repel plasma electrons. Thus, the beam splits into filaments, each of which self-pinches. However, $n_b + n_p$ remains roughly uniform at the density of immobile ions, preserving quasi-neutrality. The mode spectrum grows exponentially, in good agreement with linear theory. When n_b reaches $n_{0b} + n_{0p}$, plasma electrons are totally excluded from the filaments, and further pinching would produce strong opposing electrostatic fields. Self-pinching and linear mode growth thus end abruptly, as seen in Fig. 2, e.g., case A at $\omega_p t = 60$.

However, the essentially incompressible filaments are still subject to mutually attractive Lorentz forces, shielded by plasma return current, which flows in a sheath of thickness $\sim c/\omega_p$

outside each filament, as shown in Fig. 3. Thus, the filaments proceed to coalesce into a continually decreasing number of larger filaments, until eventually the beam recombines into a single filament, free of plasma electrons and still self-pinched to the background ion density.

The ratio of magnetic to streaming energy is

$$W_B/W_K \sim (1/N)(\nu/\gamma), \quad (3)$$

where N is the number of filaments at a given time. At the end of linear growth, $N \sim L^2/l^2$, where L is the initial beam diameter, and the mean filament separation l is essentially equal to the longest wavelength strongly represented in the spectrum, which can be estimated from linear theory. For case A, theory predicts $l \approx 2.5c/\omega_p$ and $W_B/W_K \approx 0.02$, in qualitative agreement with Fig. 1, case A, and Fig. 2. For case B, only modes with $kc/\omega_p \leq 1.6$ are unstable; consequently, filamentation occurs on a broader scale, only four filaments develop, and the linear stage continues to a larger level of W_B .

Each time filaments coalesce, W_B jumps as seen in Eq. (3) and Fig. 2, which are in qualitative agreement. The coalescing filaments bounce

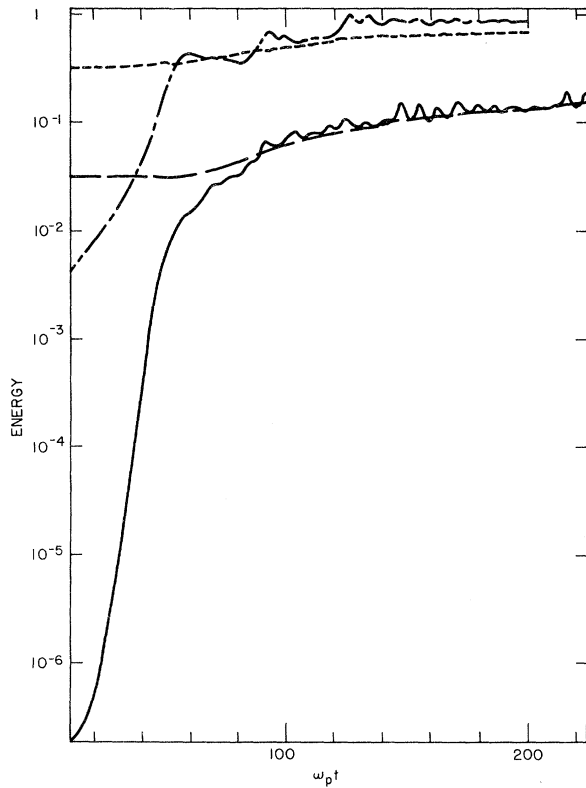


FIG. 2. Time dependence of W_B , case A, solid line; plasma thermal energy W_p , case A, long-dash line; $10W_B$, case B, dot-dash line; and $10W_p$, case B, short-dash line, all in units of the initial beam energy.

through each other in a series of damped oscillations. According to the simple picture of a test charge moving within a uniform current filament, W_B should oscillate harmonically with period $\tau_B = \pi\sqrt{2}(\gamma/\beta\omega_p) = 7.2\omega_p^{-1}$ for case A or B, in good agreement with Fig. 2.

When N finally is reduced to 1, $W_B/W_k \sim \nu/\gamma$. (Note, however, that cases A and B have been run only until $N = 2$.) The plasma is heated (mainly normal to \vec{u}_b) to an extent comparable with the increase in W_B , at least in the particular simulations done thus far (simulations varying ν/γ are in progress). Beam transverse kinetic energy also increases comparably. Thus, we expect that a beam with $\nu/\gamma \gg 1$ should divide its energy among magnetic field, plasma heating, and beam transverse energy, and fail to propagate further. It is possible that the propagation length can be adjusted by choosing B_z appropriately.

In previous one-dimensional simulations,⁴ by way of contrast, a sheet of plasma current is trapped between each pair of beam current sheets.

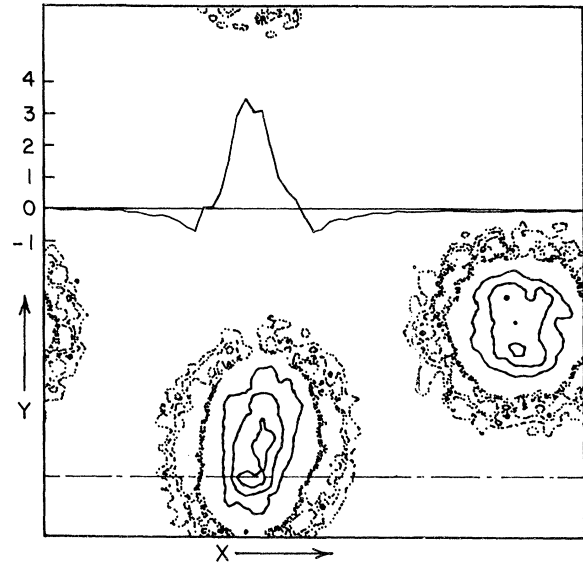


FIG. 3. Contours of total current density J_z in the plane normal to \vec{u}_b for case A at time $\omega_p t = 220$. The three solid-line contours indicate relative values $J_z = 3, 2,$ and 1 , while the dotted contours indicate $J_z = -0.4, -0.3,$ and -0.2 . The curve shown is a plot of $J_z(x)$, taken along the dot-dashed horizontal line. Note that J_z is positive within current filaments, negative in their return current sheaths, and zero elsewhere.

Thus, coalescing is impossible in one dimension, and the prevailing mode structure at the end of the linear stage persists indefinitely.⁷

Different types of structure are seen in cases C and D. In case C, the beam at first forms a connected network rather than breaking into filaments, but filamentation does occur later, and the nonlinear stage is qualitatively similar to cases A and B. In case D, where $n_{ob} = n_{op}$, distinct filamentation never occurs, although the spatial scale of the connected structure grows in the nonlinear stage until it is box limited (the analog of reduction to one filament). There is, in fact, no reason (if $n_{ob} \sim n_{op}$) why a thin neck connecting incipient filaments should be broken, since the magnetic pressure is weakest at such a point (\vec{B}_k is in the x - y plane, and the curvature is outward at a neck). A low-density beam becomes filamentous only because it shrinks to a small cross-sectional area.

It is important to note that current neutrality of the system as a whole is *not* preserved during the development of the Weibel instability of a relativistic beam. Since axial momentum $n_b m \gamma_b u_b + n_p m \gamma_p u_p$ is constant, the net current

$$I = n_b e \delta u_b (1 - \gamma_b / \gamma_p) \tag{4}$$

grows as the beam slows down. This effect characterizes any process that transfers momentum between particle streams of like charge but different effective mass. In an actual experiment in linear geometry, an equal return current is necessary to avoid charging the end plate, but typically this current can flow partially in external conductors.

During the early part of the nonlinear stage, when there are many filaments, it is qualitatively reasonable (and in moderate agreement with simulation) to treat the development statistically as continued growth of modes with long wavelength λ , $L \gtrsim \lambda \gg l$. Thus, the time scale for this stage is a few linear growth periods for modes with $\lambda \sim L$. When only a few filaments remain, such a treatment is obviously inappropriate. If each filament were fully current neutralized, the time required for coalescing of these last few filaments would become exponentially large for filament separation $\gg c/\omega_p$. However, we expect the final recombination, in an actual experiment, to be dominated by the long-range unshielded attractive force due to overall current non-neutrality. The characteristic time, i.e., the time for coalescing under this force of a pair of filaments separated by distance L , is $\tau \approx (\pi\gamma L^2/\gamma_0^2\beta^2)^{1/2} \times (1-\alpha)^{-1}\omega_p^{-1}$, where $\alpha \equiv n_{0p}u_p/n_{0b}u_b$ is the fractional current shielding. Conservation of axial canonical momentum $\vec{p}_z - e\vec{A}/c$ indicates that the change in beam momentum is $\langle \delta p_{bz} \rangle \approx (\omega_b L/4c)^2 \times N^{-1}p_0$, from which u_b and α can be estimated via Eq. (4).

The coalescing of the last few filaments is much slower than this estimate in the present simula-

tions, for two reasons. In the presence of a net current, Maxwell's equations are inconsistent with periodic boundary conditions. Thus, the code must introduce a fictitious, spatially uniform return current chosen to preserve current neutrality, negating the effect of Eq. (4). Furthermore, a periodic simulation system, unlike an actual beam of finite radius, can reach a symmetric, latticelike state. This effect dominates cases *A* and *B*. Further coalescing then depends on symmetry-breaking perturbations, and is much delayed. Therefore, the present simulations give only an upper bound on beam recombination time in a real experiment. Further simulations are in progress, involving beams with finite cross sections, and metallic rather than periodic boundary conditions.

We wish to acknowledge valuable conversations with Dr. Wallace Manheimer and Dr. H. H. Klein.

¹E. S. Weibel, Phys. Rev. Lett. **2**, 83 (1959).

²M. Bornatici and K. F. Lee, Phys. Fluids **13**, 3007 (1970).

³R. L. Morse and C. W. Nielson, Phys. Fluids **14**, 840 (1971).

⁴R. C. Davidson, D. A. Hammer, I. Haber, and C. E. Wagner, Phys. Fluids **15**, 317 (1972).

⁵G. Yonas and P. Spence, Physics International Co. Report No. PIFR-106, 1968 (unpublished). Theoretical work on other types of filamentation has been reported by G. Benford, Plasma Phys. **15**, 483 (1973).

⁶R. E. Lee, J. P. Boris, and I. Haber, Bull. Amer. Phys. Soc. **17**, 1048 (1972).

⁷These remarks apply to cold beams. In hot systems, e.g., the bi-Maxwellian Weibel, coalescing can occur in one dimension, as shown in Ref. 3.

Phonon Softening in Lanthanum under Pressure

H. Wühl, A. Eichler, and J. Wittig

Institut für Festkörperforschung der Kernforschungsanlage Jülich, D-517 Jülich, Germany

(Received 13 September 1973)

Superconducting tunneling experiments on double-hexagonal close-packed La show that the ratio $2\Delta_0/kT_c$ increases with pressure. The low-frequency part of the phonon density of states shifts to lower energies. Phonon softening is thus, at least partially, responsible for the strong increase of the superconducting T_c with pressure.

For several years the electronic structure of lanthanum metal has been a matter of unsettled controversy. Up to the present time La is often conventionally regarded as a pure *sd*-band transition metal of the third column of the periodic

table, not significantly different from scandium or yttrium.¹ On the other hand, the idea had been advanced a decade ago that a *4f* band may favorably influence the superconductivity of La.²

Experimentally, it has been shown that La is